

Self-Supporting Solid Electrolyte Based on Supramolecular Interaction for Stable Li Metal Batteries

Lixiang Guan,^[a, b] Shijun Xiao,^[a] Xiang Bai,^[b] Jiahui Zhang,^[b] Jia Su,^[b] Tiantian Lu,^[a, b] Lifeng Hou,^{*[a, b]} Huayun Du,^[a, b] Huan Wei,^[b] Xiaoda Liu,^[b] Chengkai Yang,^{*[c]} Yinghui Wie,^[a, b] and Qian Wang^{*[a, b]}

Li metal batteries based on solid polymer electrolytes offer the benefits of high energy density and safety, as well as extended cycling life, making them an excellent candidate for the next-generation battery system. However, current solid polymer electrolytes still suffer from low ion conductivity and Li⁺ transfer number, which seriously restricts its practical application. Herein, a self-supporting composite solid polymer electrolyte was prepared, where phenolic resin rich in hydroxyl groups (BR) and polyethylene oxide (PEO) are mixed evenly and poured onto a cellulose membrane in one step. In such an electrolyte, PEO and BR combine to form intermolecular hydrogen bonds,

lowering the crystallinity of PEO and increasing the Li⁺ transfer number. Lastly, the obtained solid electrolytes exhibited a high ion conductivity ($1.1 \times 10^{-4} \text{ Scm}^{-1}$) and Li⁺ transfer number (0.53), as well as improved electrochemical window. Consequently, Li || Li symmetrical cells can run stably for more than 700 h at $0.1 \text{ mA cm}^{-2}/0.25 \text{ mAh cm}^{-2}$. And full cells with LiFePO₄ cathode can also demonstrate high discharge capacity of $152.12 \text{ mAh g}^{-1}$ and rate performance. We believe that such a design based on supramolecular interaction offer a new avenue to advanced solid polymer electrolytes.

Introduction

Lithium-ion batteries (LIBs) are now commonly employed in consumer electronics and electric vehicles.^[1] However, the existing LIBs (such as: LiFePO₄ | graphite cells) is limited by their theoretical capacity of electrode materials, and its energy density is difficult to exceed 300 Wh kg^{-1} .^[2] With the continuous pursuit of LIBs with high energy density by the market/consumers, Li metal cells based on Li metal anode have been favored by researchers. Li metal anode has a high theoretical specific capacity (3860 mAh g^{-1}) and a low electrode potential (-3.04 V vs. standard hydrogen electrode), is considered to be "holy grail" among the anode materials, thus is used in various cells, such as Li-O₂ cells, Li-S cells, and Li-Ni-rich cathode cells.^[3] Furthermore, reducing the thickness of Li metal or electrolyte thickness can further improve the energy density of Li metal cells.^[4]

Nevertheless, due to its high activity, Li metal anode will chemically react with organic solvents and Li salts in liquid electrolyte to produce a solid electrolyte interface layer (SEI) on the electrode surface.^[5] The SEI layer is usually prone to deformation or even cracking during the Li plating/stripping process because of its low mechanical strength, leading to the formation/growth of Li dendrites.^[6] Severe Li dendrites are easy to pierce the separator, resulting in a short circuit in the cells, thereby creating safety hazards.^[7] Additionally, the organic liquid electrolyte is easily overconsumed during the SEI reconstruction process and is unable to effectively prevent the volume expansion of Li metal anode during cycling, which leads to low coulomb efficiency and poor cycling life.^[7b,8] In contrast, the flexible solid polymer electrolyte can enhance the interface stability between Li metal and suppress volume expansion during the Li plating/stripping process, fundamentally addressing the safety problem of organic liquid electrolytes.^[9] Finally, reducing the thickness of solid polymer electrolyte can also consequently improve the energy density, especially volumetric energy density of Li metal batteries.^[10]

Generally speaking, solid polymer electrolytes typically consists of two parts: the polymer matrix and the Li salt. The migration of lithium ions is accomplished by the recurrent "complexation-dissociation" process between the polymer chains and Li salts.^[11] At present, the most studied system is the PEO system. However, linear PEO-based solid polymer electrolyte have high crystallinity (~80%) and extremely low ionic conductivity at room temperature (~ 10^{-6} Scm^{-1}).^[9c,12] Meanwhile, the mechanical strength of PEO is poor, when the temperature exceeds 60°C , PEO is close to the molten state, the mechanical strength is poor, can not effectively inhibit the growth of lithium dendrite.^[13] And the high crystallinity of PEO results in irreversible rigidity, lowering the interface contact

[a] L. Guan, S. Xiao, T. Lu, L. Hou, H. Du, Y. Wie, Q. Wang
College of Materials Science and Engineering,
Taiyuan University of Technology,
Taiyuan, 030024, Shanxi, China
E-mail: qianwang0825@pku.edu.cn

[b] L. Guan, X. Bai, J. Zhang, J. Su, T. Lu, L. Hou, H. Du, H. Wei, X. Liu, Y. Wie, Q. Wang
Shanxi Energy Internet Research Institute,
Taiyuan, 030024, Shanxi, China

[c] C. Yang
Key Laboratory of Advanced Materials Technology,
College of Materials Science and Engineering, Fuzhou University,
350108, Fuzhou, China
E-mail: chengkai_yang@fzu.edu.cn

 Supporting information for this article is available on the WWW under
<https://doi.org/10.1002/batt.202400278>

with the electrode material. To this end, the researchers used physical compounding methods and polymer molecular design to optimize the molecular structure of PEO in order to lower the glass transition temperature (T_g) and increase the ionic conductivity. For example, Liu et al. added small molecule SN to improve the ionic conductivity of PEO at room temperature.^[14] Gerrit et al. mixed PEO and PEGDMA to prepare a cross-linked polymer electrolyte with semi-interpenetrating network, thereby improving the electrochemical performance to a certain extent, but the ionic conductivity at room temperature is still very low.^[15] In contrast, composite is an effective way to endow materials with new functions by combining functional small molecules with polymer matrix. For PEO-based solid polymer electrolytes, choosing an appropriate composite strategy is a crucial step. Typically, Zhang et al. use cellulose as the matrix materials, and compounded with PEO copolymer in a visco flow state to form fast ion channels, which significantly improved the rate and cycling performance of Li metal batteries.^[16] Similarly, Dong et al. also prepared a multifunctional polymer matrix by combining poly (methylvinyl ether-maleic anhydride) with bacterial cellulose.^[17] Therefore, it is of great significance to construct composite solid electrolyte using rigid skeleton materials.

Inspiring by the above work, we created a self-supporting composite solid electrolyte based on hydroxy-rich cellulose membrane by injecting a mixture of BR and PEO containing hydroxyl into cellulose membrane. Thanks to the supramolecular interaction (intermolecular hydrogen bonds) in the polymer matrix, the crystallinity of PEO and energy barrier of Li^+ migration are significantly reduced. Lastly, the total thickness of as-obtained composite solid electrolyte was approximately 45 μm , while it demonstrated a high Li^+ conductivity at room temperature ($1.1 \times 10^{-4} \text{ S cm}^{-1}$) and Li^+

transfer number (0.53). Consequently, the $\text{Li} || \text{Li}$ symmetrical cells can run stably for more than 600 h at 0.1 mA cm^{-2} / 0.1 mAh cm^{-2} . And the pouch cells can also undergo a series of extreme tests, such as folding and shearing, showing excellent practical application prospects.

Results and Discussion

Design Concept and Electrolyte Preparation

In order to construct a composite solid electrolyte based on strong supermolecule interactions, a cellulose membrane with a composite hydrogen bond was used as the skeleton. And the preparation process of PEO-BR composite electrolyte was shown in Figure 1a. The homogeneous solution of PEO and BR was poured into the cellulose membrane, and then formed a stable composite electrolyte after solvent evaporation. Due to the strong supramolecular interaction between PEO and BR, the crystallinity of PEO was significantly reduced and the ionic conductivity was increased.^[18] During the preparation process, we optimized the ratio of PEO and BR. As shown in Figure S1, after introducing the BR, all composite electrolytes demonstrated improved ionic conductivity and when the ratio of PEO:BR is fixed at 1:1, the ionic conductivity is maximum, ranging from $1.1 \times 10^{-4} \text{ S cm}^{-1}$ at 25°C to $3.5 \times 10^{-4} \text{ S cm}^{-1}$ at 80°C . Thus, the 1:1 was adopted the optimized ratio in subsequent electrolyte preparation, which was also consistent with our expectations after considering the interaction between hydrogen bonds. The supramolecular interactions were demonstrated by FTIR (4000–500 cm^{-1}). As shown in Figure 1b, the peak value of 1116 cm^{-1} was attributed to the vibration of $-\text{C}-\text{O}-\text{C}-$, and there was no change, indicating that the

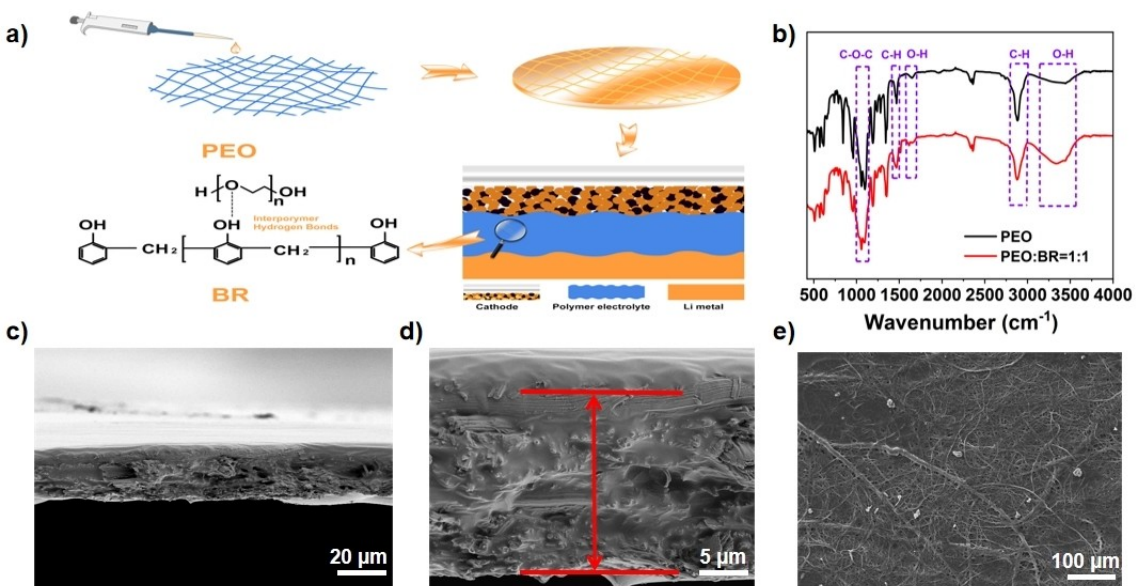


Figure 1. Synthesis scheme and characterization for composite solid polymer electrolyte. a) Schematic diagram of preparation process of electrolyte membrane; b) FTIR spectra of pure PEO electrolyte and PEO-BR composite electrolyte; c,d) Cross view of composite electrolyte at different magnifications; e) SEM image of PEO-BR composite electrolyte.

structure of PEO was not destroyed during the preparation process at high temperature.^[19] And the peak of free hydroxyl group in pure PEO was redshifted from 3523 cm^{-1} to 3415 cm^{-1} in PEO-BR composite electrolyte, means that the stretching vibration of $-\text{OH}$ was weakened, indicating that the intermolecular hydrogen bond was formed between $\text{C}-\text{O}-\text{C}$ in PEO and phenol hydroxyl group in BR. In addition, XRD was also done in this experiment, as shown in Figure S2, it can be seen that the peak decreases after the addition of BR, which further proves that PEO forms intermolecular hydrogen bonds with BR.

Then, we analyzed the thickness of the electrolyte film. As shown in Figure S3 and Figure 1c,d, the thickness of the pure PEO electrolyte is $\sim 45\text{ }\mu\text{m}$, after introducing BR, the composite electrolyte demonstrated a thickness of $\sim 50\text{ }\mu\text{m}$, has not increased significantly, which is very beneficial for improving the energy density of Li metal batteries. Meantime, there are a large number of sub-micron connected pores on the surface of the PEO-BR composite electrolyte, and the pores are evenly distributed, which is extremely favorable for the Li^+ transport (Figure 1e and Figure S4). And it can be seen from the cross view of SEM, the PEO and BR were tightly packed in the porous cellulose membrane, which is conducive to the construction of continuous ion transport channels, thereby improving the ion conductivity and Li^+ transfer number^[20] (Figure 1c,d and Figure S5). Besides, the elements C, O, S and F were uniformly distributed on the electrolyte membrane (Figure S6), suggesting that both BR and PEO were uniformly dispersed in the cellulose skeleton.

Key Electrochemical Parameters and Stability

The Li^+ migration process is usually described as the movement of polymer chains and the coupling/decoupling of Li^+ with

polar groups in the amorphous region.^[21] Therefore, it is believed that lower T_g and greater fraction of amorphous domains facilitate Li^+ migration.^[22] As shown in Figure 2a, the T_g of PEO-BR composite electrolyte is lowered to -43.5°C whereas the T_g of pure PEO electrolyte is -40.2°C . In addition, we also performed XRD experiments, as shown in Figure S2, the characteristic peaks of the composite electrolyte became smaller after the addition of BR, indicating that the supermolecule interaction between BR and PEO prevented PEO crystallization and enhanced the movement ability of PEO chains.

Ionic conductivity is one of the most important parameters for evaluating the ability of solid electrolyte to transport Li^+ . As shown in Figure 2b and Table S1, the ionic conductivity of PEO-BR composite electrolyte at room temperature can reach $1.1 \times 10^{-4}\text{ S cm}^{-1}$, which is much higher than that of pure PEO ($2.6 \times 10^{-6}\text{ S cm}^{-1}$). The increase ionic conductivity is mainly due to the supramolecular interaction between BR and PEO, which boosts the motility of the polymer chain and improves the ability to dissolve Li salts.^[23]

In addition to ion transport, electrochemical stability is also an important parameter. Here, linear sweep Voltammetry (LSV) was used to study the electrochemical stability of composite electrolyte. As shown in Figure 2c, the oxidation potential of pure PEO electrolyte is only 4.1 V , which is similar to previous reports. This is due to the fact that at high voltages, the $-\text{C}-\text{O}-\text{C}$ group on the PEO backbone is prone to oxidative decomposition. However, after introducing BR, the hydrogen bonding between BR and PEO reduces the electron cloud density of O atoms in $\text{C}-\text{O}-\text{C}$, which improves the oxidation resistance of electrolyte under high voltage, leading to the electrochemical window of composite electrolyte can be increased to 5.2 V , showing great potential in practical applications.^[24] Furthermore, we also investigated the Li^+ transfer number (t_{Li^+}) of composite electrolyte. t_{Li^+} is also a key

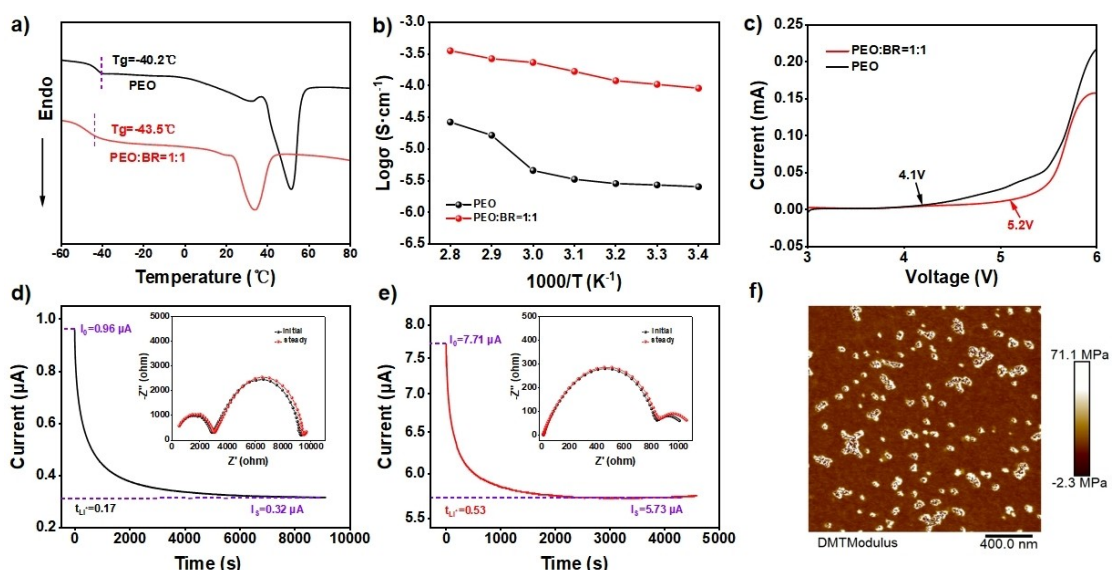


Figure 2. Key electrochemical parameters of electrolyte. a) DSC curves of pure PEO electrolyte and PEO-BR composite electrolyte; b) Ionic conductivity comparison of pure PEO electrolyte and PEO-BR composite electrolyte in the range of 25°C ~ 80°C ; c) LSV curves of pure PEO electrolyte and PEO-BR composite electrolyte; d,e) I-t curves of Li/pure PEO electrolyte/Li cell and Li/PEO-BR composite electrolyte/Li under 10 mV polarization voltage, respectively, and inset EIS before and after polarization, respectively; f) Young's modulus of PEO-BR composite electrolyte.

indicator in solid-state electrolytes, and increasing t_{Li^+} can effectively reduce the voltage polarization and increase energy output.^[25] As shown in Figure 2d,e, the pure PEO electrolyte only has a Li^+ transfer number of 0.17, whereas the PEO-BR electrolyte has a higher Li^+ transfer number of 0.53. The high t_{Li^+} also reflects that the PEO and BR combination resulted in strong intermolecular hydrogen bonds, which further reduced the crystallinity of PEO, thereby promoting the Li^+ migration. Therefore, the PEO-BR composite electrolyte can adjust the Li^+ -flux and balance the concentration polarization during charging/discharging process, improving the electrochemical performance of Li metal batteries.^[26] Furthermore, As shown in Figures 2f and S7, although the pure PEO electrolyte has a high Young's modulus at a single point, the distribution is uneven and the aggregation phenomenon is relatively serious, and the Young's modulus of the PEO-BR composite electrolyte has a more uniform distribution, which indicates that the composite electrolyte has a smooth surface and high flexibility, and it can effectively buffer the volume expansion of lithium metal anode during the charging and discharging.^[27]

In addition to electrochemical properties, thermal stability is also a key indicator. Here, TG-DSC was used to evaluate the thermal stability of PEO-BR composite electrolyte. As shown in Figure 3a, pure PEO begins to decompose rapidly at 267 °C and decomposed completely after 435 °C. However, the PEO-BR

solid polymer electrolyte lose some mass before 100 °C, owing to the presence of tiny molecules, such as acetonitrile in the manufacturing process. This tiny molecule mostly serves as a plasticizer, therefore it has little effect on the mechanical strength or electrochemical stability, and it can improve ionic conductivity at room temperature.^[28] At 310 °C, the weight loss of PEO-BR composite electrolyte becomes apparent, showing that the electrolyte has great thermal stability. Simultaneously, a high temperature heating experiment of a solid electrolyte layer using cellulose as the carrier can prove this conclusion. Furthermore, after continuous heating at 150 °C for 30 min, typical PP separator significantly crimps and deforms, whereas the composite solid electrolyte membrane retains its original shape, indicating that the electrolyte membrane with cellulose as the carrier has excellent thermal stability, which improves the safety of Li metal batteries (Figure 3b).

In addition, symmetric cells were assembled to compare the interface compatibility and long-term stability between PEO-BR composite electrolyte and Li metal anode. For interface compatibility, as shown in Figure 3c, with increasing temperature, the interface impedance steadily decreased. The compatibility with the electrode interface is improved due to the gradual transformation of the polymer into a molten state. It is worth noting that the overall interface resistance is relatively small, especially at 40 °C, below 200 Ω , indicating fast ion

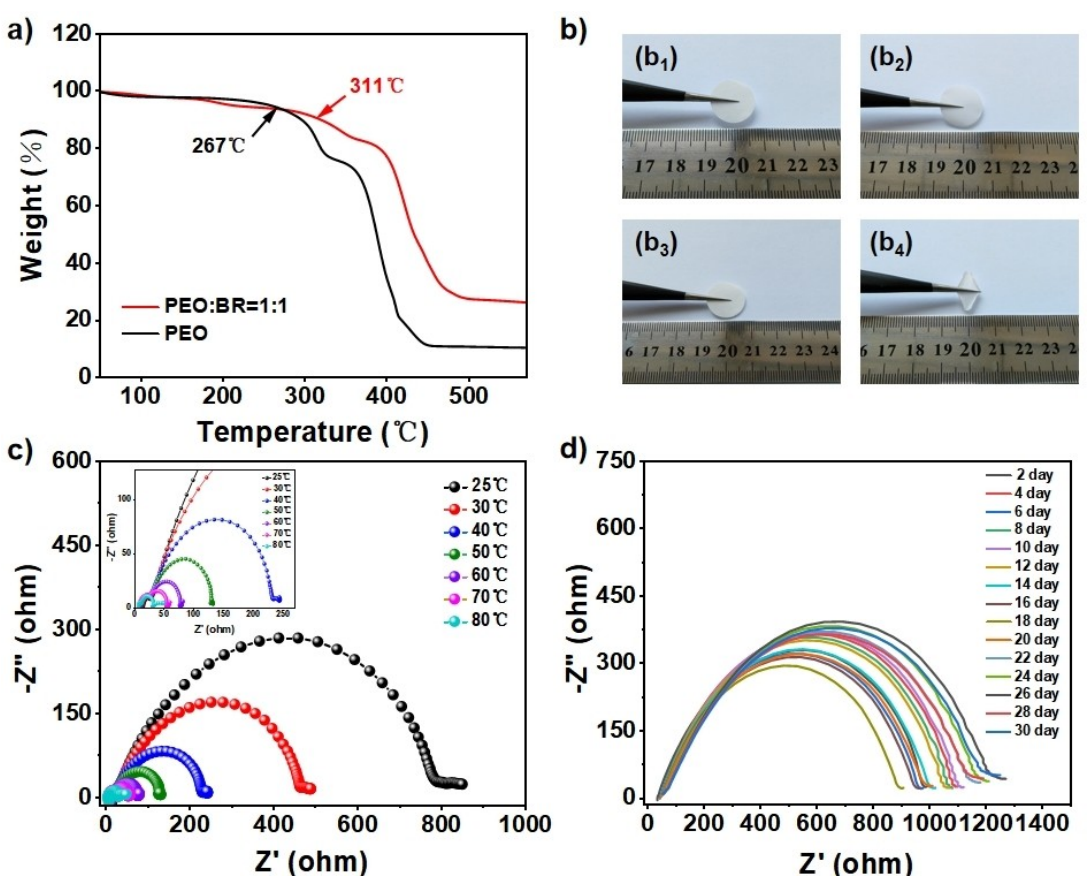


Figure 3. Stability of composite electrolyte. a) TGA curves of pure PEO electrolyte and PEO-BR electrolyte; b) Optical photos of (b₁ and b₃) solid electrolyte film and (b₂ and b₄) PP separator before and after holding at 150 °C for 30 min; (b₁–b₂) before heating; (b₃–b₄) after heating; c) EIS spectra of Li/PEO-BR electrolyte/Li cell at different temperatures (test interval 30 min), d) EIS spectra of Li/PEO-BR electrolyte/Li cell at different times.

transfer characteristics.^[29] For long-term stability, Figure 3d reveal that while the PEO-BR electrolyte continues to react with the Li metal, the interface resistance rises. After 14 days, however, the impedance falls to a somewhat steady value, indicating a stable SEI layer. After 28 days, the electrical resistance remained constant, showing that the PEO-BR electrolyte has excellent interfacial compatibility with Li metal.^[30]

Electrochemical Performance

Symmetrical Cells and Post Analysis

To further evaluate the application potential of PEO-BR composite electrolyte in Li metal batteries, we conducted Li plating/stripping tests to study its voltage polarization and interface stability. As shown in Figure 4a, when the current density was fixed at 0.1 mA cm^{-2} and the surface capacity was 0.1 mAh cm^{-2} , the Li/PEO-BR /Li cells still maintained a stable voltage platform after 600 h, and the polarization voltage was only 140 mV, implying that there was a stable interface. In contrast, when pure PEO electrolyte was used, the overpotential was significantly higher than that of the PEO-BR composite electrolyte. This suggests that the pure PEO electrolyte undergoes an irreversible chemical interaction with Li metal, causing in a rise in interface impedance and, finally, the short circuit phenomena in the symmetric cells after ~ 200 h. In order to further verify the advancement of supramolecular interaction on the PEO-BR electrolyte, a deeper Li plating/stripping tests was performed, which was shown in Figure S8. When the capacity of Li plating/stripping was increased to 0.25 mAh cm^{-2} , the Li/PEO-BR/Li cell can be stable for more than 700 h. This suggests that the supramolecular force in the PEO-BR electro-

lyte inhibits the formation of Li dendrites and stabilizes the electrode/electrolyte interface, thereby improving the cycling stability.

The morphology of Li electrodes after cycling was also investigated. As shown in Figure 4b,c and Figure S9, the cell with PEO electrolyte has uneven Li surface after cycling due to low ion transport and poor interface compatibility. And uneven Li deposition eventually forms a large amount of "dead Li". In contrast, when using PEO-BR electrolyte, the Li surface after cycling exhibited a smooth surface without "dead Li", which can be attributed the strong supramolecular interaction between BR and PEO, improving the ionic conductivity and the Li^{+} transfer number, thereby regulating Li^{+} -flux and ensuring uniform Li deposition.^[31] Besides, we also compared the electrolyte surface after cycling by AFM (Figure 4d and 4e and Figure S10). The roughness of the initial electrolyte film was reduced from 3.1 μm of PEO to 37.2 nm of PEO-BR, showing that the addition of BR reduced the roughness and enhanced the compatibility between the electrolyte film and the electrode. After cycling, the roughness of the PEO-BR film grew to 404.7 nm, which was considerably lower than that of the PEO membrane, implying that the composite electrolyte membrane had higher interfacial compatibility.

Full Cells and Application

To demonstrate the potential of PEO-BR electrolytes for practical high-performance all-solid-state Li metal batteries, we assembled LiFePO₄/PEO-BR SPE/Li full cells. As shown in Figure 5a,b, the discharge capacities of LFP/PEO-BR SPE/Li cells at current densities of 0.1C, 0.2C and 0.5C were $152.12 \text{ mAh g}^{-1}$, $142.63 \text{ mAh g}^{-1}$ and $100.85 \text{ mAh g}^{-1}$, respectively. When the

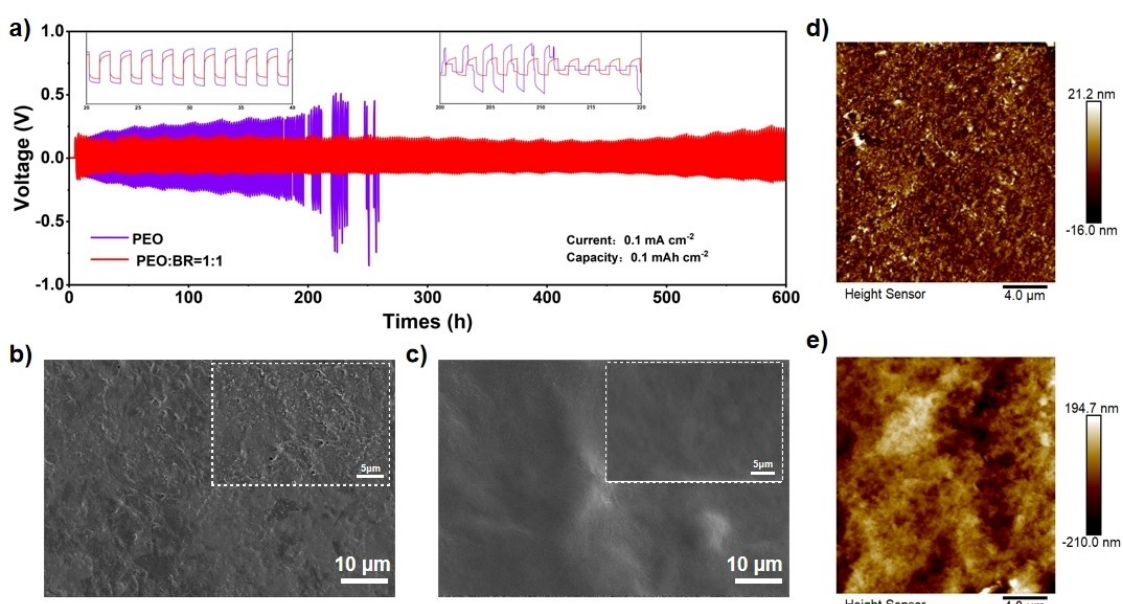


Figure 4. Symmetrical cells and post analysis. a) Long-term Li plating/stripping experiment for symmetric cells with composite electrolyte at the current density of $0.1 \text{ mA cm}^{-2}/0.1 \text{ mAh cm}^{-2}$. The illustrations are potential distribution at different stages. b,c) SEM images of Li metal surface after cycling of Li/pure PEO/Li and Li/PEO-BR SPE/Li symmetric cells, respectively. d,e) AFM images comparison of pure PEO (e) and PEO-BR composite electrolyte (d) after cycling.

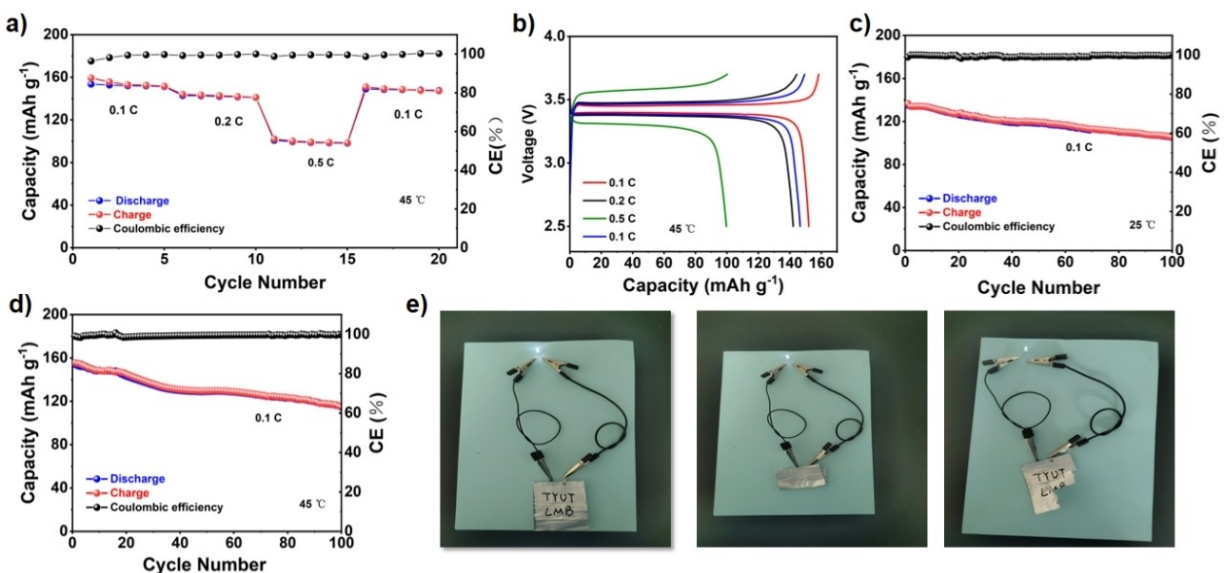


Figure 5. Full cells and pouch cells. a) Rate capability and Coulomb efficiency of LFP/PEO-BR SPE/Li cells; b) Charging and discharging curves at different current densities; c, d) Long cycle performance at 0.1 C, 25 °C (c) and 45 °C (d); e) LFP/PEO-BR SPE/Li pouch cells in folded, first cut, second cut for LED power.

current density was switched back to 0.1 C, the discharge capacity was restored to 148.61 mAh g⁻¹, indicating that the PEO-BR electrolyte has excellent cyclic reversibility. Besides, it can be seen from Figure 5b, the overall low overpotential indicates that the interface between the PEO-BR electrolyte and the electrodes was kept good contact, which was conducive to the half cells. Subsequently, we performed a long cycle test at 0.1 C to evaluate the cycling stability. As shown in Figure 5c, the full cells displayed an initial discharge capacity of 135.11 mAh g⁻¹, and after 100 cycles, the capacity retention rate was ~80%. When the full cells were run at 45 °C, the cells also exhibited a high discharge capacity of 152.01 mAh g⁻¹ and a coulombic efficiency consistently above 99%. Because high temperatures increase the motility of the polymer chain, the ionic conductivity of the polymer electrolyte, and the contact between the electrolyte and the electrode, the interface compatibility improves.^[32] Subsequently, the full cells were disassembled after 100 cycles and the Li metal surface was characterized by SEM (Figures S11 and S12). After 100 cycles, the electrolyte surface has no obvious cracks, indicating that the composite electrolyte has excellent mechanical and cyclic stability.

Further, we also assembled a simple pouch cell. As shown in Figure 5e, the full cells exhibited a stable discharge voltage and can continuously light up LED small bulbs. In addition, after a series of destructive tests such as: folding and shearing, the pouch cell did not experience smoke or short circuits, and the small light bulb could still be lit for a long time, proving that the composite electrolyte has high safety.

Finally, this work also used a high nickel positive electrode (NCM811) to assemble a full battery, as shown in Figure S13 and S14, which has a stable charge/discharge curve with a discharge specific capacity of up to 168.1 mAh g⁻¹ at a current

density of 0.1 C, and a stable cycling at a high current density of 0.5 C, which is promising for a wide range of applications.

Conclusions

In summary, we provided a composite electrolyte based on supramolecular interaction employing cellulose as a carrier. The PEO and BR can form a strong intermolecular hydrogen bond, which increases the amount of amorphous area and hinders PEO crystallization, thereby improving the ionic conductivity and Li⁺ transfer number. As a result, thanks to the supramolecular interaction, the composite electrolyte demonstrated a high ionic conductivity of 1.1×10⁻⁴ Scm⁻¹ and Li⁺ transfer number was increased from 1.7 to 5.3. Meanwhile, the composite electrolyte displayed good interface compatibility and stability, leading to the symmetrical cell can cycle stably for more than 600 h at 0.1 mA cm⁻²/0.1 mAh cm⁻². The full cells with LFP cathode can also run stably for 100 cycles with high coulomb efficiency. And pouch cells can also withstand a series of extreme tests, such as folding and shearing, demonstrating excellent practical application prospects.

Supporting Information

Supporting Information is available from the Wiley Online Library or from the author.

Author Contributions

Lixiang Guan: Conceptualization, Methodology, Writing – original draft, Investigation, Data curation. **Shijun Xiao:** Inves-

tigation, Validation. **Xiang Bai**: Investigation, Validation. **Jiahui Zhang**: Investigation, Validation. **Jia Su**: Investigation, Validation. **Tiantian Lu**: Investigation, Validation. **Lifeng Hou**: Supervision, Resources, Project administration. **Huayun Du**: Supervision, Resources. **huan Wei**: Supervision, Resources. **Xiaoda Liu**: Supervision, Resources. **Chengkai Yang**: Supervision, Resources. **Yinghui Wei**: Supervision, Resources, Project administration. **Qian Wang**: Supervision, Formal analysis.

Acknowledgements

This work was supported by the National Natural Science Foundation of China (No. 52071227), the Beijing Natural Science Foundation-Xiaomi innovation joint Foundation (L223011), Key Scientific Research Project in Shanxi Province (Grant No. 201805D121003), Special Found Projects for Central Government Guidance to Local Science and Technology Development, Science and Technology Major Projects of Shanxi Province (20191102004), Young Elite Scientists Sponsorship Program by CAST (2022QNRC001), Fundamental Research Program of Shanxi Province (202103021222006), Shanxi Energy Internet Research Institute (SXEI2023A004), Young Elite Scientists Sponsorship Program by CAST (2022QNRC001), (2019D111102), Research Project Supported by Shanxi Scholarship Council of China (HGKY2019085).

Conflict of Interests

The authors declare no conflict of interest.

Data Availability Statement

The data that support the findings of this study are available from the corresponding author upon reasonable request.

Keywords: Li metal anode · dendrites · solid polymer electrolyte · supramolecular interaction · Li metal batteries

- [1] a) Q. Wang, T. Lu, Y. Liu, J. Dai, L. Guan, L. Hou, H. Du, H. Wei, X. Liu, X. Han, Z. Ye, D. Zhang, Y. Wei, H. Zhou, *Energy Storage Mater.* **2023**, *55*, 782; b) X. Yu, A. Manthiram, *Energy Storage Mater.* **2021**, *34*, 282; c) Z. Wang, L. Shen, S. Deng, P. Cui, X. Yao, *Adv. Mater.* **2021**, *33*, 2100353; d) H. Huang, D. Li, L. Hou, H. Du, H. Wei, X. Liu, Q. Wang, Y. Wei, *J. Power Sources* **2022**, 542.
- [2] a) Y. Liu, B. Xu, W. Zhang, L. Li, Y. Lin, C. Nan, *Small* **2020**, *16*, e1902813; b) Q. Wang, S. Wang, T. Lu, L. Guan, L. Hou, H. Du, H. Wei, X. Liu, Y. Wei, H. Zhou, *Adv. Sci.* **2022**, *10*, e2205233; c) W. Tang, G. Zhou, J. Cao, Z. Chen, Z. Yang, H. Huang, Y. Qu, C. Li, W. Zhang, H. Liu, *ACS Appl. Energ. Mater.* **2021**, *4*, 2962.
- [3] a) Q. Wang, P. Zou, L. Ren, S. Wang, Y. Wang, Z. Huang, Z. Hou, Z. Jiang, X. Lu, T. Lu, L. Guan, L. Hou, C. Yang, W. Liu, Y. Wei, *Adv. Funct. Mater.* **2023**, *33*, 2213648; b) P. Fan, H. Liu, V. Marosz, N. T. Samuels, S. L. Suib, L. Sun, L. Liao, *Adv. Funct. Mater.* **2021**, *31*, 2101380.
- [4] C. Sun, J. Liu, Y. Gong, D. P. Wilkinson, J. Zhang, *Nano Energy* **2017**, *33*, 363.

- [5] a) G. Xi, M. Xiao, S. Wang, D. Han, Y. Li, Y. Meng, *Adv. Funct. Mater.* **2020**, *31*, 2007598; b) F. Xu, S. Deng, Q. Guo, D. Zhou, X. Yao, *Small Methods* **2021**, *5*, 2100262.
- [6] J. Wang, K. Wang, Y. Xu, *ACS Nano* **2021**, *15*, 19026.
- [7] a) Q. Liu, A. Cresce, M. Schroeder, K. Xu, D. Mu, B. Wu, L. Shi, F. Wu, *Energy Storage Mater.* **2019**, *17*, 366; b) Q. Guo, F. Xu, L. Shen, S. Deng, Z. Wang, M. Li, X. Yao, *Energy Material Advances* **2022**, *2022*, 9753506.
- [8] a) C.-Z. Zhao, B.-C. Zhao, C. Yan, X.-Q. Zhang, J.-Q. Huang, Y. Mo, X. Xu, H. Li, Q. Zhang, *Energy Storage Mater.* **2020**, *24*, 75; b) Z. Liang, G. Zheng, C. Liu, N. Liu, W. Li, K. Yan, H. Yao, P. C. Hsu, S. Chu, Y. Cui, *Nano Lett.* **2015**, *15*, 2910.
- [9] a) L. Han, L. Wang, Z. Chen, Y. Kan, Y. Hu, H. Zhang, X. He, *Adv. Funct. Mater.* **2023**, *33*, 202300892; b) Q. Guo, F. Xu, L. Shen, Z. Wang, J. Wang, H. He, X. Yao, *J. Power Sources* **2021**, *498*, 229934; c) Z. Wang, Q. Guo, R. Jiang, S. Deng, J. Ma, P. Cui, X. Yao, *Chem. Eng. J.* **2022**, *435*, 135106; d) X. Zhao, X. Kong, G. Li, Y. Zhao, Z. Jia, F. He, P. Yang, K. Ge, M. Zhang, Z. Liu, *Fuel* **2024**, *360*, 130605.
- [10] a) R. Chen, W. Qu, X. Guo, L. Li, F. Wu, *Mater. Horiz.* **2016**, *3*, 487; b) L. Long, S. Wang, M. Xiao, Y. Meng, *J. Mater. Chem. A* **2016**, *4*, 10038.
- [11] a) C. Xian, Q. Wang, Y. Xia, F. Cao, S. Shen, Y. Zhang, M. Chen, Y. Zhong, J. Zhang, X. He, X. Xia, W. Zhang, J. Tu, *Small* **2023**, *19*, e2208164; b) P. L. Kuo, C. A. Wu, C. Y. Lu, C. H. Tsao, C. H. Hsu, S. S. Hou, *ACS Appl. Mater. Interfaces* **2014**, *6*, 3156.
- [12] D. He, S. Y. Cho, D. W. Kim, C. Lee, Y. Kang, *Macromolecules* **2012**, *45*, 7931.
- [13] M. W. Schulze, L. D. McIntosh, M. A. Hillmyer, T. P. Lodge, *Nano Lett.* **2014**, *14*, 122.
- [14] Y. Yang, C. Liu, Z. Lv, H. Yang, Y. Zhang, M. Ye, L. Chen, J. Zhao, C. C. Li, *Adv. Mater.* **2021**, *33*, e2007388.
- [15] G. Homann, L. Stoltz, M. Winter, J. Kasnatscheew, *iScience* **2020**, *23*, 101225.
- [16] J. Zhang, C. Ma, Q. Xia, J. Liu, Z. Ding, M. Xu, L. Chen, W. Wei, *J. Membr. Sci.* **2016**, *497*, 259.
- [17] T. Dong, J. Zhang, G. Xu, J. Chai, H. Du, L. Wang, H. Wen, X. Zang, A. Du, Q. Jia, X. Zhou, G. Cui, *Energy Environ. Sci.* **2018**, *11*, 1197.
- [18] J. Ryu, S. Kim, J. Kim, S. Park, S. Lee, S. Yoo, J. Kim, N. S. Choi, J. H. Ryu, S. Park, *Adv. Funct. Mater.* **2019**, *30*, 1908433.
- [19] S. Yang, Z. Liu, Y. Liu, Y. Jiao, *J. Mater. Sci.* **2014**, *50*, 1544.
- [20] X. Shen, H. Liu, X.-B. Cheng, C. Yan, J.-Q. Huang, *Energy Storage Mater.* **2018**, *12*, 161.
- [21] A. Varzi, R. Raccichini, S. Passerini, B. Scrosati, *J. Mater. Chem. A* **2016**, *4*, 17251.
- [22] a) S. M. Hao, S. Liang, C. D. Sewell, Z. Li, C. Zhu, J. Xu, Z. Lin, *Nano Lett.* **2021**, *21*, 7435; b) L. Chen, W. Li, L. Z. Fan, C. W. Nan, Q. Zhang, *Adv. Funct. Mater.* **2019**, *29*, 1901047.
- [23] C. Zheng, Y. Lu, Q. Chang, Z. Song, T. Xiu, J. Jin, M. E. Badding, Z. Wen, *Adv. Funct. Mater.* **2023**, *33*, 2302729.
- [24] Z. A. Ghazi, Z. Sun, C. Sun, F. Qi, B. An, F. Li, H. M. Cheng, *Small* **2019**, *15*, e1900687.
- [25] a) Y. Kondo, T. Abe, Y. Yamada, *ACS Appl. Mater. Interfaces* **2022**, *14*, 22706; b) H.-B. Han, K. Liu, S.-W. Feng, S.-S. Zhou, W.-F. Feng, J. Nie, H. Li, X.-J. Huang, H. Matsumoto, M. Armand, Z.-B. Zhou, *Electrochim. Acta* **2010**, *55*, 7134.
- [26] Q. Wang, H. Zhang, Z. Cui, Q. Zhou, X. Shangguan, S. Tian, X. Zhou, G. Cui, *Energy Storage Mater.* **2019**, *23*, 466.
- [27] M. T. McDowell, I. Ryu, S. W. Lee, C. Wang, W. D. Nix, Y. Cui, *Adv. Mater.* **2012**, *24*, 6034.
- [28] X. Zhu, K. Wang, Y. Xu, G. Zhang, S. Li, C. Li, X. Zhang, X. Sun, X. Ge, Y. Ma, *Energy Storage Mater.* **2021**, *36*, 291.
- [29] S.-K. Jung, H. Gwon, G. Yoon, L. J. Miara, V. Lacivita, J.-S. Kim, *ACS Energy Lett.* **2021**, *6*, 2006.
- [30] Q. Liu, Y. Liu, X. Jiao, Z. Song, M. Sadd, X. Xu, A. Matic, S. Xiong, J. Song, *Energy Storage Mater.* **2019**, *23*, 105.
- [31] E. Adhitama, A. D. Refino, T. Brake, J. Pleie, C. Schmidt, F. Demelash, K. Neuhaus, S. Bornemann, S. Wiemers-Meyer, E. Peiner, M. Winter, H. S. Wasisto, T. Placke, *J. Mater. Chem. A* **2023**, *11*, 7724.
- [32] B. Liu, K. Fu, Y. Gong, C. Yang, Y. Yao, Y. Wang, C. Wang, Y. Kuang, G. Pastel, H. Xie, E. D. Wachsman, L. Hu, *Nano Lett.* **2017**, *17*, 4917.

Manuscript received: April 25, 2024

Revised manuscript received: May 8, 2024

Accepted manuscript online: May 11, 2024

Version of record online: June 24, 2024